NTU Journal of Engineering and Technology (2023) 2 (2) : 7-15
DOI: https://doi.org/10.56286/ntujet.v2i2.483

IRAQI Academic Scientific Journals

P-ISSN: 2788-9971 E-ISSN: 2788-998X
NTU Journal of Engineering and Technology
Available online at: https://journals.ntu.edu.iq/index.php/NTU-JET/index

STUDYING OF DUAL DEEP PERIOCULAR PARTS FOR PERSONS RECOGNITION

Safa N. H. Al-Moktar[1], Raid Rafi Omar Al-Nima[2]
1. College of Basic Education, University of Mosul, Mosul, Iraq
2. Technical Engineering College / Mosul, Northern Technical University, Iraq, E-mail: raidrafi1@gmail.com

Article Informations

Received: 04-04- 2023,
Revised: 24-05-2023
Accepted: 01-06-2023,
Published Online: 17-10-2023

Corresponding author:
Name: Safa N. H. Al-Moktar
Affiliation : University of Mosul,
Email: raidrafi1@gmail.com

Key Words:
Deep Learning,
Periocular,
Recognition.

A B S T R A C T

Recently, periocular region has been employed in recognitions and it can be so effective especially in wearing a face mask as happened during the Coronavirus pandemic. In this study, a new method is proposed for recognizing persons based on their perioculars. It is named the Dual Deep Periocular Parts (DDPP). In this method, two deep learning networks are employed, where each network is determined for a certain periocular side (right or left). They are termed the Deep Network for the Right Periocular (DNRP) and Deep Network for the Left Periocular (DNLP). Both the DNRP and DNLP are fused together to construct the proposed DDPP approach. Also in this paper, a database called the Northern Technical University Periocular Database (NTUPD) is collected from scratch. Persons recognition based on the proposed periocular approach shows further performance enhancements as we obtained results of accuracy that reached 98.7% and Equal Error Rate (EER) 1.3%.

1. INTRODUCTION

1.1. Overview

The name of "biometrics" refers to "life measurements". That is, it actually refers to the use of a person's distinctive traits for recognitions. It utilizes a person's physiological traits or behavioral traits such as irisprint, retina patterns, fingerprints, facial geometry, voices and signatures [1].

There are a wide range of biometric systems such as face identification, iris recognition, fingerprint authentication, finger vein verification and voice identity.

1.2. Biometric Requirements

Before confirming any trait as a biometric, a number of requirements must be met. Internationality, permanence, individuality and measurability are examples of fundamental factors to be taken into accounts [2]. Fundamental factors or requirements can be illustrated as follows [3]:

- Internationality: The biometric should be accessible to all people.
- Permanently: It refers to the biometric's stability for long life.
- Individuality: It refers to biometric's ability to be recognizable for anyone.
- Measurability: This emphasizes the capability of measuring the biometric.

1.3. Biometric Types

In general, biometrics can be divided into two types as follows [4]:

a) Physiological: it is a type of characteristics that points to a part of a person's body such as fingerprint, iris print, ear print and Deoxyribonucleic Acid (DNA).

b) Behavioral: it is a type of characteristics which indicates a person's behavior such as gait, keystroke and signature.

Behavioral biometrics are influenced by emotional states as illness or tension. On the other hand, physiological biometrics are often more precise, stronger and consistent [5]. In this study, a physiological biometric of periocular is considered.

1.4. Study Aim

The study aim is recognizing persons based on their periocular biometric.

1.5. Study Contributions

The contributions of this study can be listed as follows:

- Partitioning periocular region into right and left sides.
- Providing a Deep Network for the Right Periocular (DNRP).
- Providing a Deep Network for the Left Periocular (DNLP).
- Proposing the Dual Deep Periocular Parts (DDPP), which benefits from the DNRP and DNLP.

2. GENERAL BACKGROUND ON PERIOCULAR BIOMETRIC

2.1. General Background

The region of the face that surrounds the eyes is known as the periocular. The prefix "peri-" means "around or about" and the root word "ocular" means "of or connected to the eye". Such phrase has been used in biometrics to refer to both tiny area such as the eyes, eyelids and lashes, and a broader area such as the eyebrow [6]. Basically, the first study that was introduced the periocular region to be used as a biometric was in 2009 [7]. After that, such region was investigated more in other studies.

Area surrounding the eyes, which is known as periocular region, is very feature-rich and it includes elements like eyelids, eyelashes, eyebrows, tear ducts, eye shape, skin texture and many more. Given that face and iris based biometrics provide significant levels of recognitions, periocular region can afford good substitutions [8].

2.2. Periocular Area

It has been cited that the size of periocular window has a greater impact on recognition performance. It also found that while too big window may consider worthless features, too small window may not include some useful features. Examples of periocular Region of Interests (ROIs) extracted from a face image is shown in figure 2.1 [9].

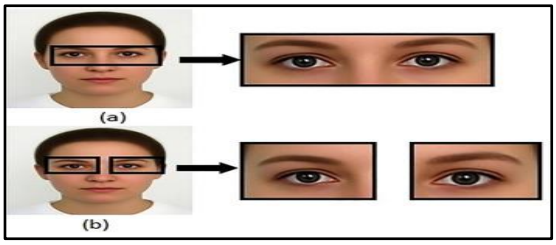

Figure 2.1. Examples of periocular ROIs extracted from a face image

Lower eyelids, sclera, skin tone, texture, blood vessels, tear ducts, inner corner, outer corner, eyelashes and eyelids are some typical components of periocular region that can be identified simply. The eye centers make suitable candidates because they can be recognized from periocular images with significant position variations, whereas other important spots are obscured by attitude changes [10].

Important features for a periocular image of one eye is given in figure 2.2 [9].

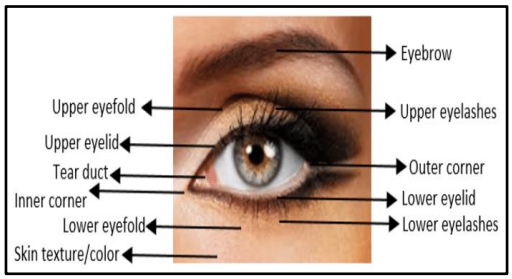

Figure 2.2. Important features for a periocular image of one eye

Facial region can be scaled, rotated and cropped to a predetermined size as a part of the alignment procedure so that the eye centers are horizontally aligned and positioned on typical locations. Whole picture alignment procedure for an example image is shown in figure 2.3 [10].

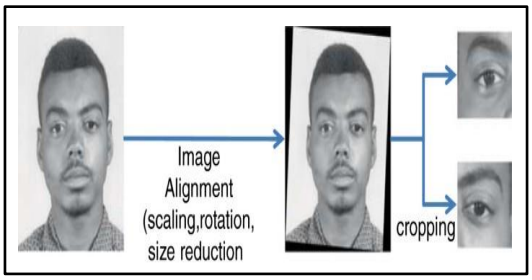

Figure 2.3. Image alignment and periocular extractions of the two eyes from a face image

2.3. Advantages of Periocular Biometric

Periocular biometric has substantial advantages that can be highlighted as follows:

- ❖ It does not require a high resolution and extensive camera to capture its image.
- ❖ It can have friendly acquisition due to its contactless nature.
- ❖ It is so useful with wearing masks than the face biometric, where masks are used for protecting from viruses infections such as the Corona virus.
- ❖ Since its biometric is distinct, using it can be considered better than utilizing Identity (ID) cards and passwords. This is because the ID card and password may be lost, forgotten, stolen or given to an unauthorized person.
- ❖ It does not influenced by emotional states as illnesses or tensions as behavioral biometrics.

2.4. Previous Studies

Different previous studies for periocular recognitions are provided as follows:

In 2008, Mandal *et al.* illustrated that periocular region is a subset of the facial region which includes eyes as well as the area in the vicinity of eyes. This includes regions such as eyes, eye lashes, eyebrows, cheek and skin texture. This study considered personal identification [11].

In 2009, Park *et al.* described the area of the right face around the eye. In contrast to other ocular biometrics (such as iris, retina, and sclera), periocular biometric acquisition does not require near capturing distance and significant user cooperation. Using texture and point operators, global and local information were extracted from the periocular region producing a feature set that can be matched. The work was also done with the results of combining these sets of features. Using 958 photos taken from 30 different participants, the experimental results demonstrated 77% of identification accuracy [12].

In the same year, Park *et al.* cited that periocular-based recognition has attracted more and more attentions by biometric researchers. Gradient orientation, Local Binary Pattern (LBP) and Scale-Invariant Feature Transform (SIFT) were the three descriptors which were provided. The periocular recognition method outperformed face recognition under occlusion in the experimental comparisons [13].

In 2010, Woodard *et al.* explained that the likelihood of human recognition in unrestricted contexts is greatly increased by utilizing both irises and periocular texture simultaneously. Periocular data could be collected using only the iris camera as there were no other sensors required for acquisition. It has been confirmed that information about eye shape and skin texture around it can differ between individuals and be used as a soft biometric [14].

In the same year, Park *et al.* introduced the idea of periocular recognition and identified people by using their peripheral visions. It has been made clear that the iris serves as supplemental information which can be used from a distance and the face is an invariant region [15].

In 2011, Juefei-Xu *et al.* carried out an experiment to analyze the feasibility of periocular region according to the age invariants. The Face and Gesture Recognition Network (FG-NET) was used. For pose correction and illumination, a normalization method, pre-existing active appearance model and anisotropic diffusion model were respectively applied. With Walsh-Hadamard Transform (WHT) encoded lipopolysaccharide-binding protein LBP as a feature descriptor and Unsupervised Discriminant Projection (UDP) for subspace modelling, identification rate was obtained 100% and verification rate was attained 98% at 0.1% False Acceptance Rate (FAR) [16].

In 2012, Padole *et al.* examined the performance of a periocular-based recognition system. The authors investigated the effects of scale, position, occlusion, … etc. on the performance of a periocular-based recognition system and came to the conclusion that recognition system performance suffers by presence of such covariates [17].

In 2014, Nie *et al.* used periocular imaging for automated and precise biometric identification. There were varieties of use, from enhancing iris recognition system performance to monitoring people, especially, with less limited imaging

environments. A Convolutional variation of Restricted Boltzman Machines (CRBM) was designed to support high picture sizes and significantly lessen computational load. The purpose of this study was to examine new methods for periocular biometric recognition that can be more useful for identifying human subjects in great databases [18].

In 2016, Raja *et al.* examined the performance of periocular biometrics for the images obtained before and after plastic surgery of near-by regions of eyes. A database was applied for several shapes and texture feature descriptors. An identification rate of 53.73% was obtained. Based on the lower identification accuracy it was concluded that the surgical changes degrade the performance of periocular biometrics and this issue needs further investigations [19].

In the same year, Juefei-Xu *et al.* illustrated that one of the most real-world difficulties in biometrics is recognizing a suspect who is wearing a mask (when just periocular region is visible). This is a significant issue that arises frequently in law enforcement applications. In this study, a method for reconstructing the full frontal face utilizing only periocular area was suggested. The effectiveness of the face reconstruction method was empirically demonstrated, it was based on modified sparsifying dictionary learning algorithm [20].

In 2017, Proença *et al.* claimed that discarding of ocular components like sclera and iris from periocular region could optimize the recognition accuracy. To justify such claim, a large set of multiclass samples was created by interchanging the periocular and ocular parts of different images captured from two databases. Images were employed as inputs to Alexnet Convolutional Neural Network (CNN) model. Recognition accuracy of 88% and 92% were achieved for the two employed databases [21].

In 2018, Juefei-Xu *et al.* claimed that periocular region is a very rich featured region in the face. They developed a dictionary learning approach known as Dimensionality Weighted K-Singular Value Decomposition (DWKSVD) method. Sparse representation of the periocular image was firstly obtained using the Orthogonal Matching Persuit (OMP) and then the whole face was reconstructed using the face components of the DW-KSVD dictionary. For analyzing the performance of the reconstructed face and its matching with the original face, the described method was re-implemented and obtained a verification accuracy of 82.6%. This showed that periocular region could be considered as a good option to be used instead of the full face via the DWKSVD without losing too much verification accuracy [21].

In 2019, Behera *et al.* suggested a recognition system used for cross-spectral matching of periocular images. It has shown a case where the gallery and probe consisted of visible and Near Infra-Red (NIR) images, respectively. The first step involved pre-processing, where the images are processed in order to mitigate the effect of illumination and appearance variations. The pre-possessed images were then fed to the feature extraction in order to extract local or global descriptors. The gallery and probe images were then compared using distance metrics in order to get normalized matching scores in the range between 0 to 1, where 0 means no match at all and 1 means a full match. Either the matching scores or the probability scores could be compared with a threshold to finally determine whether the probe was for a genuine user or an imposter [22].

In 2020, Alahmadi *et al.* proposed a simple, efficient and compact image representation technique that takes into account the wealth of information and sparsity existing in the activations of the convolutional layers. Principle component analysis was employed. Pertained CNN model of Very Deep Convolutional Networks (VGG-Net) was used. For recognition, an efficient and robust Sparse Augmented Collaborative Representation based Classification (SA-CRC) technique was utilized. Obtained results showed the superiority of the proposed Convert Sample Rate Converter (Conv SRC) over the state-of-the-art methods, where it obtained a Global Medical Response (GMR) of more than 99% at Forced Migration Review (FMR) = 10^{-3} [23].

In 2023, Sharma *et al.* clarified that the presence of masks, as what happened with Corona Virus Disease 2019 (COVID-19) pandemic, and other types of facial coverings may affect the performance of face recognition systems. In this article, detailed review of periocular biometric was presented. Various face and periocular methods specifically created to identify people hiding their faces were essed. Aspects of periocular biometrics were provided including: (a) periocular region's anatomical cues that are helpful for recognition, (b) various developed feature extraction and matching techniques, (c) recognition across different spectra, (d) fusion with other biometric modalities, (e) recognition using on mobile devices, (f) usefulness in applications, and (g) databases [24].

From the literature review, it can be noticed that some studies worked on the periocular biometric by using deep learning techniques. In this study, additional deep learning contribution will be provided for the periocular biometric and increasing its recognition performance.

3. METHODOLOGY

3.1. Deep Learning

Deep learning is a type of machine learning that enables computers to learn from experience and comprehend the environment in terms of a hierarchy of concepts. It covers relevant mathematical concepts in the areas of probability, information

theory, and linear algebra. likewise, machine learning is used in applications such as natural language processing, speech recognition, computer vision, online recommendation systems, bioinformatics and video games [25]. There are different types of deep learning networks such as the CNN, Recurrent Neural Networks (RNN) and Generative Adversarial Network (GAN).CNN is widely employed to address numerous image analyses issues in various fields as medical imaging, healthcare, self-driving automobiles, virtual assistant, entertainment industry, fraud detection, natural language processing and visual recognition [26]. This kind of networks is suitable to be utilized in this study as it has the capability to efficiently analyze and recognize images of periocular. It includes the following layers: 1st convolution, 1st Rectified Linear Unit (ReLU), 1st pooling, 2nd convolution, 2nd ReLU, 2nd pooling, …, FC, softmax and classification. Such architecture can be seen in figure 3.1 [27].

In the convolution layer, an input image is convolved with kernels to get feature maps. Then, the ReLU layer rectified the negative values to zeros and produces updated feature maps.

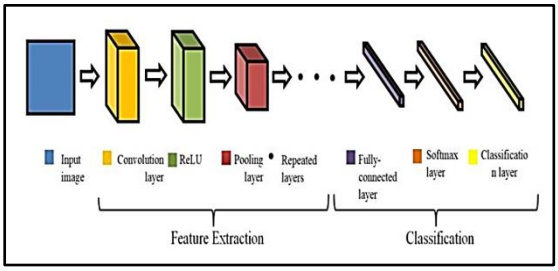

Figure 3.1. General CNN architecture

After that, the resulted feature maps are treated with pooling layers to reduce their spatial sizes. This process is repeated for the number of times and accordingly different feature extractions are provided. Consequently, the last resulted feature maps from the last pooling layer are matched to a Fully Connected (FC) layer, which starts a classifier to get outputs of image recognition. Hence, softmax layer shows confidence scores for all output classes. Finally, the classification layer is exploited to perform the last decision according to the softmax layer confidence scores [27].

3.2. Proposed Approach

An approach called the DDPP is proposed in this study. It involves two deep learning networks named the DNRP and DNLP, both are based on the CNN. Basically, the left periocular side and right periocular side for the same person are separately used in this work. The results of both sides are combined together as this can increase recognition performance. Figure 3.2 shows general block diagram of the proposed approach.

The main deep learning network that is employed in this study for each of the DNRP and DNLP is based on the CNN, where it consists of the essential CNN layers. These are the: input layer, convolution layer, ReLU layer, pooling layer, FC layer, softmax layer and classification layer.

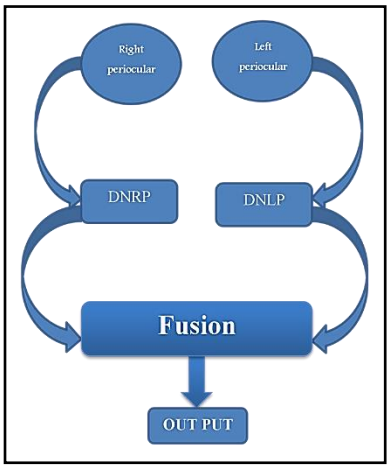

Figure 3.2. General block diagram of the proposed DDPP

3.2.1. *Input Layer*

The input layer has been adapted to a periocular side image. It accepts a colored squared image **E** of three channels: one for red $\mathbf{E}^r$, one for green $\mathbf{E}^g$ and one for blue $\mathbf{E}^b$.

3.2.2. *Convolution Layer*

Each channel of the input image **E** is analyzed into feature maps in this layer, where a kernel matrix and input channel are convolved to create the feature map.

$$z_{u,v,c^l} = B_{c^l} + \sum_{i=-k_h^l}^{k_h^l} \sum_{j=-k_w^l}^{k_w^l} \sum_{c^{l-1}=1}^{c^{l-1}} W_{i+k_h^l, j+k_w^l, c^{l-1}}^{c^l} z_{u+i,v+j,c^{l-1}} \quad (3.1)$$

where z_{u,v,c^l} is the output of the convolution layer, (u, v) is a given pixel, c^l is a channel of the current layer, l is the current layer, B_{c^l} is a channel bias, k_h^l and k_w^l are respectively the kernel height and kernel width of a channel, $l-1$ is the previous layer, and $W_{i+k_h^l, j+k_w^l, c^{l-1}}^{c^l}$ is the kernel parameter [28].

3.2.3. *ReLU Layer*

This layer implements the ReLU activation function. It can provide the non-linear calculations to the deep learning network. It keeps the positive values and rectifies the negative values to zeros according to the following equation:

$$O_{u,v,c^l} = max(0, z_{u,v,c^l}) \quad (3.2)$$

where O_{u,v,c^l} is the output of a ReLU node and max is the maximum operation [29].

3.2.4. Pooling Layer

The pooling layer reduces the sizes of the ReLU channels. It collected the maximum or average values of feature maps from the previous layer. In general, maximum pooling type can be implemented according to the following equation:

$$q_{a^l,b^l,c} = \max_{0\le a<p_h,0\le b<p_w} o_a^l \times p_h + a, b^l \times p_w + b, c \quad (3.3)$$

where $q_{a^l,b^l,c}$ is the output of a pooling node, max is for the maximum value, $0 \le a^l < p_h^l$, p_h^l is the height of a pooled feature map, $0 \le b^l < p_w^l$, p_w^l is the width of a pooled feature map, $0 \le c < c^l = c^{l-1}$, and p_h and p_w are respectively the height and width of feature map sub regions that need to be pooled [30].

Average pooling type calculates the average values for patches of feature maps and creates down-sampled (pooled) feature maps. It extracts features more smoothly than the maximum pooling type [31][32]. The following equation expresses the average pooling operation:

$$q_{a^l,b^l,c} = \operatorname{average}_{0\le a<p_h,0\le b<p_w} o_a^l \times p_h + a, b^l \times p_w + b, c \quad (3.4)$$

where average is for the average value.

3.2.5. *FC Layer*

FC layer is used to match between the number of required recognized classes and number of pooling nodes. The generated channels in layer $l-1$ are re-mapped as $m_1^{l-1} \times m_2^{l-1} \times m_3^{l-1}$ dimensional vectors according to the following equation:

$$g_r = \sum_{a=1}^{m_1^{l-1}} \sum_{b=1}^{m_2^{l-1}} \sum_{c=1}^{m_3^{l-1}} w_{a,b,c,d,r}^l (Q_C)_{a,b,} \forall 1 \le r \le m^l \quad (3.5)$$

where g_r is the output of a FC node, m_1^{l-1} is the height of a previous layer channel, m_2^{l-1} is the width of a previous layer channel, m_3^{l-1} is the number of produced channels in the previous layer, $w_{a,b,c,d,r}^l$ is the connection weights between the FC and pooling layers, Q_C is the vector or vectors of pooling layer outputs, and m^l the number of the required recognized classes [33].

3.2.6. *Softmax Layer*

This layer considers the softmax activation function, where it utilizes to calculate the relationship probabilities between the input and each output class. It uses the following equation:

$$y_r = \frac{\exp(g_r)}{\sum_{s=1}^{m_1^{l-1}} \exp(g_s)} \quad (3.6)$$

where y_r is the output of a softmax node [33].

3.2.7. *Classification Layer*

Lastly, the classification layer is exploited to perform the decision. This layer follows a winner-takes-all rule. This rule can be represented by the following equation:

$$D_r = \begin{cases} 1 & \text{if } y_r = \max \\ 0 & \text{otherwise} \end{cases}, r = 1,2,3,\dots n \quad (3.7)$$

where D_r is the output decision of a classification node, max is the maximum y_r value and n is the number of classes [4].

3.3. Dual Fusion

In this study, a dual fusion between the two deep learning networks of the DNRP and DNLP is proposed and implemented, it is named the DDPP. The right periocular and left periocular images are used as inputs. The outputs of the two employed deep learning networks are merged together according to a certain rule. There are various types of fusion rules as AND, NAND, OR, NOR, XOR and XNOR rules. It has been approved that the OR rule can lead to obtain a high accuracy [34][35], as is also investigated [36]. So, it is adopted.

4. RESULTS AND DISCUSSIONS

4.1. Database Description

A database of periocular images was collected from scratch. It is named the Norther Technical University Periocular Database (NTUPD). A large number of periocular images were collected. It consists of 850 images for 70 persons. Camera of a resolution 8 Megapixels for a smartphone of type (Galaxy A50) was utilized. Its auto focus was on, whilst, its flash was off at times of capturing periocular images. Also, different backgrounds and lighting environments were used. Images were collected from September 2022 to December 2022. Volunteers of both genders and various ages (from 4 to 60 years old) were participated in this database. Each volunteer participated by 10 to 12 images for his/her periocular region. Many of them were students in the University of Mosul / College of Basic Education. All taken pictures are colored of type Joint Photographic Experts Group (JPEG).

4.2. Characteristics of Deep Leaning Networks

As mentioned, the network architecture of each DNRP and DNLP networks is suggested to utilize the main CNN layers. Figure 4.1 shows the suggested network architecture for each of the DNRP and DNLP.

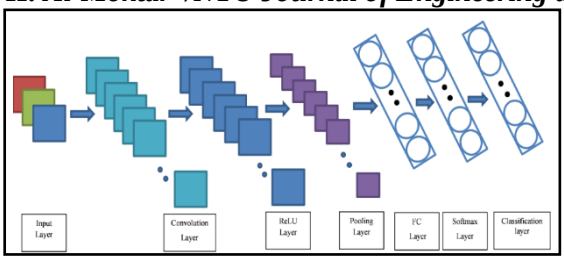

Figure 4.1. Suggested network architecture for each of the DNRP and DNLP

Deep learning characteristics for each of the employed DNRP and DNLP networks are as follows: input image size equal to 50 × 100 × 3 pixels, convolution layer of filter size equal to 5 × 5 pixels, number of convolution filters equal to 20, convolution stride equal to 1 × 1 pixels for both horizontal and vertical directions, convolution padding size equal to 0 around all borders of input channels, pooling of average type, pooling window size of 2 × 2 pixels, stride value equal to 2× 2 pixels for both horizontal and vertical directions, pooling padding size equal to 0 around all borders of input channels, number of FC layer nodes equal to 70, number of softmax layer nodes equal to 70, and number of classification layer nodes equal to 70.

4.3. Computer Specifications and Training Options:

All experiments are conducted to a computer which has the following specifications: laptop of type Lenovo, processor of type Core-i5, processor speed of 2.7GHz and main memory of size 4 Giga Bytes.

For training options, the following settings are used: stochastic gradient descent with momentum optimizer, momentum = 0.9, fixed learn rate = 0.0001, weight decay = 0.0001, mini batch size = 128 and maximum epochs = 30.

4.4. Results and Discussions for Training:

First of all, 70% of periocular images from the NTUPD database is randomly used for training purposes. Training curves for the DNRP network is given in figure 4.2. Whereas, training curves for the DNLP network is shown in figure 4.3.

Two curves can be seen in each figure. Blue curve shows relationship between training accuracy and number of iterations. Whilst, red curve provides relationship between the loss function and number of iterations. All curves indicate the successfulness of training. Obviously, accuracies have been successfully raised and errors have been reasonably reduced for training both the DNRP and DNLP networks.

4.5. Results and Discussions for Testing:

First of all, 30% of periocular images from the NTUPD database is randomly used for testing purposes. For testing both the DNRP and DNLP, table 4.1 shows performances of both networks in the cases of accuracy and Equal Error Rate (EER).

This table shows that persons recognition performance for right sides of periocular images attain slightly higher than left sides. That is, the suggested DNRP network achieves accuracy of 90.04% and EER of 9.96%, whereas, the DNLP obtains accuracy of 87.45% and EER of 12.55%. This means that periocular region has rich of features and any periocular side part can provide recognition. Furthermore, both periocular sides may achieve near results.

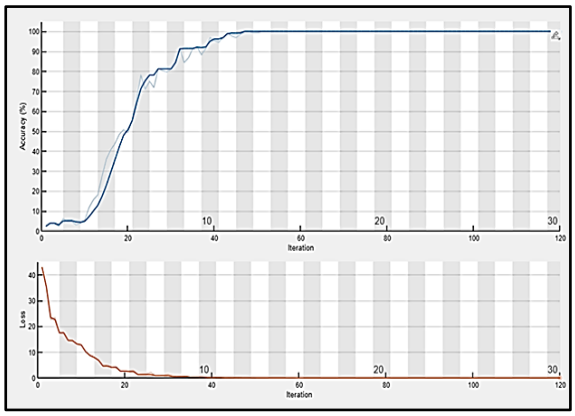

Figure 4.2. Training curves for the DNRP network

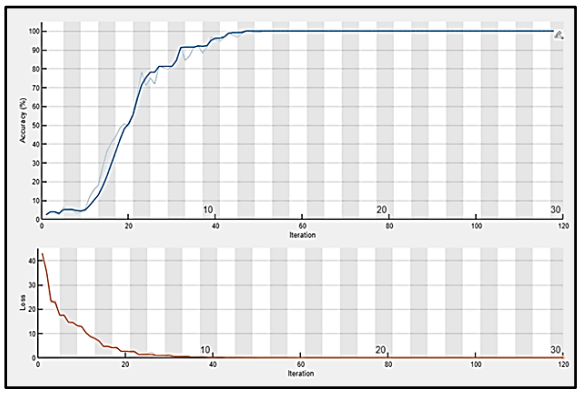

Figure 4.3. Training curves for the DNLP network

Table 4.1. Performances of both networks in the cases of accuracy and EER

DL Network	Accuracy	EER
DNLP	87.45%	12.55%
DNRP	90.04%	9.96%

For the DDPP approach, various fusion rules have been evaluated. Table 4.2 shows performance comparison between different fusion rules of the NOR, XOR, NAND, AND, XNOR and OR (the rules are arranged according to their performances).

Table 4.2 is clearly yielded that chosen rule can affect obtained performances. NOR fusion rule attains worst accuracy of 1.29% and worst EER of 98.71%. XOR rule obtains low accuracy of 19.91% and high EER of 80.09%. NAND fusion rule achieves closer performance to the XOR rule, where accuracy reports 20.77% and EER reports 79.23%.

AND fusion rule attains comparable accuracy of 79.22% and comparable EER of 20.78%. XNOR rule obtains closer performance to the AND fusion rule, where accuracy reports 80.09% and EER reports 19.91%. Finally, the OR rule benchmarks highest accuracy of 98.68% and lowest EER of 1.32%. Therefore, the OR fusion rule is selected to be employed in the DDPP approach.

Table 4.2. Comparisons between different fusion rules

Fusion Rule	Accuracy	EER
NOR	1.29%	98.71%
XOR	19.91%	80.09%
NAND	20.77%	79.23%
AND	79.22%	20.78%
XNOR	80.09%	19.91%
OR	98.68%	1.32%

It can be highlighted that applying only one deep learning network (based on the CNN) may not lead to obtain high performance. On the other hand, applying fusions between multiple deep learning networks to parts of periocular areas can surely be more valuable to attain very high results. This rates the DDPP contribution of this paper in the cases of its scientific strength and quality to the field of recognition based on the periocular.

5. CONCLUSIONS

In this study, the main aim is recognizing persons based on their periocular biometrics. A new DDPP approach was proposed. It utilized two deep learning networks. They termed the DNRP and DNLP. DNRP was used for the right periocular side and the DNLP was utilized for the left periocular side. The outcomes of the DNRP and DNLP are fused for the proposed DDPP.

NTUPD database was collected from scratch, it contains 850 colored image from 70 people of different ages and for both genders. The NTUPD database were randomly divided into 70% of periocular images for training purposes and 30% of periocular images for testing purposes.

The DDPP was evaluated for various fusion rules. The OR rule proves its effectiveness of providing the highest performance. That is, the DDPP approach showed a very high recognition accuracy of 98.68% and a very low EER value of 1.30%.

REFERENCES

[1] Pato, J. N., & Millett, L. I. (2010). Cultural, Social, and Legal Considerations. In: Biometric Recognition: Challenges and Opportunities. National Academies Press.

[2] Jain, A. K. Bolle, R., & Pankanti, S. (2006). BIOMETRICS: Personal Identification in Networked Society. in *Biometrics*, Boston, MA: Springer US. doi: 10.1007/0-306-47044-6_10.

[3] Jain, A. K., Ross, A. A., & Prabhakar, S. (2004). An Introduction to Biometric Recognition. *IEEE Transactions on Circuits and Systems for Video Technology*. doi: 10.1109/TCSVT.2003.818349.

[4] Al-Nima, R. R. O. (2017). Signal Processing and Machine Learning Techniques for Human Verification Based on Finger Textures. PhD thesis, Newcastle University, UK.

[5] Wei, H. (2007). An integrated and distributed biometric-based user authentication architecture. Dissertation University of Ottawa (Canada),.

[6] Park, U. Jillela, R. R., Ross, A., & Jain, A. K. (2010). Periocular biometrics in the visible spectrum. *IEEE Transactions on Information Forensics and Security*, 6(1).

[7] Park, U., Ross, A., & Jain, A. K. (2009). Periocular biometrics in the visible spectrum: A feasibility study. *IEEE 3rd international conference on biometrics: theory, applications, and systems*, IEEE.

[8] Snir, R. (2011). Computer and information sciences. *Journal of King Saud University*.

[9] ALGASHAAM, F. M. NGUYEN, K. CHANDRAN, V., & BANKS, J. (2017). Elliptical higher-order-spectra periocular code. IEEE Access 5.

[10] Mahalingam, G., & Ricanek, K. (2013). LBP-based periocular recognition on challenging face datasets. *EURASIP Journal on Image and Video processing*.

[11] Mandal, B. Jiang, X., & Kot, A. (2008). Verification of human faces using predicted eigenvalues. *19th International Conference on Pattern Recognition*, IEEE.

[12] Park, U., Ross, A., & Jain, Anil K. (2009). Periocular biometrics in the visible spectrum: A feasibility study. *IEEE 3rd international conference on biometrics: theory, applications, and systems.*

[13] Park, U. Ross, A., & Jain, A. K. (2009). Periocular biometrics in the visible spectrum: A feasibility study. *IEEE 3rd international conference on biometrics: theory, applications, and systems.*

[14] Woodard, D. L., Pundlik, S., Miller, P., Jillela, R., & Ross, A. (2010). On the fusion of periocular and iris biometrics in non-ideal imagery. *20th International Conference on Pattern Recognition*, IEEE.

[15] Park, U., Jillela, R. R., Ross, A., & Jain, A. K. (2010). Periocular biometrics in the visible spectrum. *IEEE Transactions on Information Forensics and Security*, 6(1).

[16] Juefei-Xu, F., Luu, K., Savvides, M., Bui, T. D., & Suen, C. Y. (2011). Investigating age invariant face recognition based on periocular biometrics.

International Joint Conference on Biometrics (IJCB), IEEE.

[17] Padole, C. N., & Proenca, H. (2012). Periocular recognition: Analysis of performance degradation factors. *2012 5th IAPR international conference on biometrics (ICB)*, IEEE.

[18] Nie, L., Kumar, A., & Zhan, S. (2014). Periocular recognition using unsupervised convolutional RBM feature learning. *22nd International Conference on Pattern Recognition*, IEEE.

[19] Raja, K., Raghavendra, R., & Busch, C. (2016). Biometric recognition of surgically altered periocular region: A comprehensive study. *International Conference on Biometrics (ICB)*, IEEE.

[20] Juefei-Xu, F., Pal, D. K., & Savvides, M. (2014). Hallucinating the full face from the periocular region via dimensionally weighted K-SVD. *Proceedings of the IEEE Conference on Computer Vision and Pattern Recognition Workshops*.

[21] Proenca, H., & Neves, J. C. (2017). Deep-prwis: Periocular recognition without the iris and sclera using deep learning frameworks. *IEEE Transactions on Information Forensics and Security*, 13(4).

[22] Behera, S. S. Mandal, B., & Puhan, N. B. (2019). Cross-spectral periocular recognition: A survey. *Emerging Research in Electronics, Computer Science and Technology*, Springer, Singapore.

[23] Alahmadia, A., Hussaina, M., Aboalsamha, H., & Zuaira, M. (2020). ConvSRC: SmartPhone-based periocular recognition using deep convolutional neural network and sparsity augmented collaborative representation. *Journal of Intelligent & Fuzzy Systems*, 38(3).

[24] Sharmaa, R., & Ross, A. (2023). Periocular biometrics and its relevance to partially masked faces: A survey. *Computer Vision and Image Understanding*.

[25] Goodfellow, I., Bengio, Y., & Courville, A. (2016). Deep learning. MIT press.

[26] Sarvamangala, D. R., & Kulkarni, R. V. (2021). Grading ofKnee Osteoarthritis Using Convolutional Neural Networks. *Neural Processing Letters*, 53(4).

[27] AL-Hatab, M. M., Al-Nima, R. R. O., Marcantoni, I., Porcaro, C., & Burattini, L. (2020). Classifying Various Brain Activities by Exploiting Deep Learning Techniques and Genetic Algorithm Fusion Method. *TEST Engineering & Management*, 83.

[28] Simo-Serra, E., Iizuka, S., Sasaki, K., & Ishikawa, H. (2016). Learning to simplify: fully convolutional networks for rough sketch cleanup. *ACM Transactions on Graphics (TOG)*, 35(4).

[29] Stein, C., Nickel, C., & Busch, C. (2012). Fingerphoto recognition with smartphone cameras. *BIOSIG-Proceedings of the International Conference of Biometrics Special Interest Group (BIOSIG)*, IEEE.

[30] Wu, J. (2017). Introduction to convolutional neural networks. National Key Lab for Novel Software Technology, Nanjing University, China, 5(23).

[31] Tolias, G., Sicre, R., & J´egou, H. (2015). Particular object retrieval with integral max-pooling of CNN activations. *arXiv preprint arXiv:1511.05879*.

[32] Razavian, A. S., Sullivan, J., Carlsson, S., & Maki, A. (2016). Visual instance retrieval with deep convolutional networks. *ITE Transactions on Media Technology and Applications*, 4(3).

[33] Stutz, D. (2014). Neural codes for image retrieval. *Proceeding of the Computer Vision-ECCV*.

[34] Al-Nima, R. R. O., Hasan, S. Q., & Esmail, S. (2020). Exploiting the Deep Learning with Fingerphotos to Recognize People. *International Journal of Advance Science and Technology*, 29(7).

[35] Al-Nima, R. R. O., Hasan, S. Q., Mahmood, S. E. (2023). Utilizing Fingerphotos with Deep Learning Techniques to Recognize Individuals. *NTU Journal of Engineering and Technology*, 2(1), pp. 39-45.

[36] Al-Nima, R. R., Han, T., Chen, T., Dlay, S., & Chambers, J. (2020). Finger texture biometric characteristic: a survey. *arXiv preprint arXiv:2006.04193*.